PHYSICAL REVIEW B VOLUME 36, NUMBER 14 15 NOVEMBER 1987-I

Elastic behavior under hydrostatic pressure and acoustic-mode vibrational anharmonicity of single-crystal berlinite

H. A. A. Sidek,* G. A. Saunders, and Wang Hong†
School of Physics, University of Bath, Claverton Down, Bath, BA2 7AY, United Kingdom

Xu Bin and Han Jianru
Institute of Crystal Materials, Shandong University, Jinan Shandong, People's Republic of China

(Received 27 March 1987)

The set of the second-order elastic constants and their hydrostatic-pressure derivatives have been obtained for the rhombohedral single-crystal berlinite ($AlPO_4$) using the ultrasonic pulse echo overlap technique. To quantify the vibrational anharmonicity, the acoustic-mode Grüneisen parameters in the long-wavelength limit have been derived in the quasiharmonic approximation. The results extend previous observations that the elastic and physical behavior of berlinite is quite similar to that of quartz. The hydrostatic-pressure derivative $\partial C_{66}/\partial P$ has a negative value indicating that the corresponding transverse-acoustic mode softens under pressure; this is in accord with the anomalous positive temperature dependence of C_{66}. The anomalous behavior of C_{66} indicates that there may be even at room-temperature influence of the zone-center optic phonon, whose softening is associated with the α-β structural transformation, on long-wavelength transverse-acoustic phonons propagating in the same crystallographic direction.

INTRODUCTION

Several oxides with the composition $A^{\mathrm{III}}B^{\mathrm{V}}O_4$ exist in structures which can be considered as a derivative of isoelectronic quartz SiO_2, constructed by replacing half the Si atoms by A^{III} and the other half by B^{V}.[1] Aluminum phosphate, $AlPO_4$, in its rhombohedral modification berlinite belongs to the same point group (32) in the trigonal $R1$ crystal system as quartz and so is noncentrosymmetric and piezoelectric. The structural relationship between the two materials is close[2] and many similarities between their physical properties have been pointed out: elastic properties,[3–5] piezoelectric properties,[5] surface-acoustic-wave (SAW) velocities.[6] Berlinite also resembles quartz in many of its other low- and high-temperature properties such as density, hardness, refractive indices.[7] Quartz is used in many electronic devices based on bulk acoustic, surface acoustic, and surface-skimming bulk wave technologies. Berlinite has a larger piezoelectric coupling coefficient than quartz: There is considerable interest in its potential for technological applications. Device design will rely upon knowledge of the fundamental physical properties including the elastic constants and their behavior with pressure.

The second-order elastic constants (SOEC's) of berlinite have been measured previously using several different techniques, including ultrasonic pulse superposition,[4] ultrasonic pulse-echo overlap,[3] and the resonance method.[5,8] Considerable differences occur between the various data sets. Temperature-dependence measurements of the SOEC's[3] show that the elastic constants, except C_{66} and C_{14}, decrease in the normal way with increasing temperature. This unusual behavior of C_{66} and C_{14} resembles that in quartz, although the temperature derivatives of the SOEC's of berlinite are less than half those of quartz. No previous information on the effects of hydrostatic pressure on the lattice-dynamical behavior is available for berlinite. Hence the central objective in the present program has been to study the elastic behavior under pressure and to quantify the acoustic-mode vibrational anharmonicity which is approached here by reference in the mode Grüneisen parameters. The slopes of the acoustic branch of phonon dispersion curves at the Brillouin-zone center are directly related to the elastic constants[9] and the pressure derivatives of the elastic constants quantify the pressure-induced changes in these slopes. A decrease in an elastic constant under the influence of pressure can indicate incipient lattice instability because it corresponds to a reduction in crystal stiffness to the particular acoustic-phonon mode.[10] At about 853 K berlinite (the trigonal α form of $AlPO_4$) undergoes a structural transformation to the hexagonal β form,[11] a transition which is associated with softening of a zone-center optic phonon.[12–15] The finding here of a negative pressure derivative for C_{66} indicates that even at room temperature there could be a degree of interaction between the soft optic phonon and the transverse-acoustic phonon in the same crystallographic direction leading to the anomalous behavior of C_{66} with pressure.

EXPERIMENTAL PROCEDURE AND RESULTS

Good optical-quality single crystals of berlinite ($AlPO_4$) were grown using a slow-heating technique in an autoclave using methods described elsewhere.[16] The defects in these crystals have been characterized by optical and scanning electron microscopy and by their effects on electrical properties.[5] To determine the crystal orientation needed for ultrasonic-wave propagation, the Laue x-ray backreflection method has been employed. To specify the elastic moduli without ambiguity and relate them to other physical properties, in particular the phonon dispersion curves, it is necessary to define the crystallographic axial set with respect to the atomic arrangement in the crystal in which the measurements are made. This has been achieved by following the IRE standards on piezoelectric crystals;[17] the Z axis parallel to the optic axis, the X axis parallel to one of the three binary axes (normal to the Z axis), and the Y axis completes the right-handed orthogonal axial set.

Several specimens with pairs of faces parallel to better than 10^{-4} radians were cut and polished. The cuts prepared include X, Y, Z cuts and one off axis (see Table I for the directions selected for ultrasonic wave propagation). The density of berlinite was determined using the liquid-immersion technique as $2.652 \pm 0.020\ \mathrm{g\,cm^{-3}}$. This is in reasonable agreement with results of other workers $2.620\ \mathrm{g\,cm^{-3}}$ using the same technique, $2.618\ \mathrm{g\,cm^{-3}}$ by the x-ray powder method;[18] the density reported by Mason[8] was $2.566\ \mathrm{g\,cm^{-3}}$.

To obtain the ultrasonic-wave velocities (Table II), the transit time of a 10-MHz ultrasonic pulse was measured by the pulse-echo overlap technique.[19] X- and Y-cut quartz transducers were attached to the specimen with Dow Resin 276-V9. The six independent elastic constants (Tables III and IV) have been obtained from measurements made on six modes (2, 3, 7, 8, 9, 10) which do not involve a piezoelectric contribution, and so are referred to as unstiffened modes. There are considerable discrepancies between published sets of elastic constants for berlinite (Table III). Hence it was considered necessary to make an extensive series of measurements to resolve this problem. The mean elastic constants obtained are compared with those of other workers in Table III. The results lie close to the data sets given by Refs. 3 and 4 and can be considered as providing confirmation of those measurements. The values of C_{11}, C_{33}, C_{12}, and C_{44} measured here lie between those obtained by those two groups of workers. There is substantial scatter in the values of C_{13}; our own value of C_{13} being a little larger than that given in Ref. 4. That of C_{66} is slightly smaller than those given in Refs. 3 and 4. The source of much of the difference between the elastic-constant sets probably stems from the difficulty of preparing high-quality berlinite crystals; each group of workers would have been working with crystals having different defect structures. Workers seeking a set of elastic constants may be advised to use a weighted average ($C_{11}=6.5$, $C_{12}=0.90$, $C_{13}=1.24$, $C_{14}=-1.24$, $C_{33}=8.72$, $C_{44}=4.31$, $C_{66}=2.86$ in units of $10^{10}\ \mathrm{N\,m^{-2}}$) of those given in Refs. 3 and 4 and the present data.

However, the present aim of measurement of the hydrostatic-pressure derivatives of the elastic constants necessitates use of the actual ultrasonic-pulse transit times obtained on our own crystals to provide a basis for determining the relative effects on wave velocity induced by hydrostatic pressure, and this has been done.

Hydrostatic-pressure dependences (Fig. 1) up to 3×10^8 Pa were made in a piston and cylinder apparatus using Plexol 201 as the pressure-transmitting media. To bypass the requirement of calculation of the change in crystal dimensions under hydrostatic stress, the concept of "natural velocity" W (Ref. 24) has been used. The

TABLE I. The effective second-order elastic constants (C_{ij}) of berlinite. Y′/+45° designates a propagation direction in the $(+Y+Z)$ plane at an angle of 45° to the $+Y$ axis. $\underset{\sim}{e}$ is the piezoelectric tensor and $\underset{\sim}{\epsilon}$ is the effective dielectric tensor. $e'_{26}=-(e_{11}+e_{14})/2$, $e''_{26}=-(e_{11}-e_{14})/2$, $\epsilon'_{22}=(\epsilon_{11}+\epsilon_{33})/2$, L denotes longitudinal, FS denotes fast shear, SS denotes slow shear, S denotes shear, QL denotes quasi-longitudinal, QS denotes quasi-shear, $C_{ij}=C_{ij}^E$, $\epsilon_{ij}=\epsilon_{ij}^S$.

No.	N	U	Mode	ρW^2
1	X	X	L	$C_{11}+e_{11}^2/\epsilon_{11}$
2	X	Y	FS	$(C_{66}+C_{44})/2+[(C_{66}-C_{44})^2+4C_{14}^2]^{1/2}/2$
3	X	Z	SS	$(C_{66}+C_{44})/2-[(C_{66}-C_{44})^2+4C_{14}^2]^{1/2}/2$
4	Y	Y	QL	$(C_{44}+C_{11})/2+[(C_{44}-C_{11})^2+4C_{14}^2]^{1/2}/2$
5	Y	Z	QS	$(C_{44}+C_{11})/2-[(C_{44}-C_{11})^2+4C_{14}^2]^{1/2}/2$
6	Y	X	S	$C_{66}+e_{11}^2/\epsilon_{11}$
7	Z	Z	L	C_{33}
8	Z	Y	S	C_{44}
9	Y′/+45°	Y′	QL	$(C_{11}+C_{33}+2C_{44}-2C_{14})/4$ $+[(C_{11}-C_{33}-2C_{14})^2/4+(C_{44}+C_{13}-C_{14})^2]^{1/2}/2$
10	Y′/+45°	Z′	QS	$(C_{11}+C_{33}+2C_{44}-2C_{14})/4$ $-[(C_{11}-C_{33}-2C_{14})^2/4+(C_{44}+C_{13}-C_{14})^2]^{1/2}/2$
11	Y′/+45°	X	S	$(C_{44}+C_{66}+2C_{14})/2+(e'_{26})^2/\epsilon'_{22}$
12	Y′/−45°	Y′	QL	$(C_{11}+C_{33}+2C_{44}-2C_{14})/4$ $+[(C_{11}-C_{33}-2C_{14})^2/4+(C_{44}+C_{13}-C_{14})^2]^{1/2}/2$
13	Y′/−45°	Z′	QS	$(C_{11}+C_{33}+2C_{44}-2C_{14})/4$ $-[(C_{11}-C_{33}-2C_{14})^2/4+(C_{44}+C_{13}-C_{14})^2]^{1/2}/2$
14	Y′/−45°	X	S	$(C_{44}+C_{66}-2C_{14})/2+(e''_{26})^2/\epsilon'_{22}$

TABLE II. Natural wave velocity W (units $\mathrm{m\,s^{-1}}$), the initial slope $(\rho_0 W^2)'$ of the hydrostatic-pressure dependence, and the elastic modulus $(\rho_0 W^2)$ (units 10^{10} $\mathrm{N\,m^{-2}}$) for each ultrasonic mode (nomenclature given in Table I) propagated in berlinite at 298 K.

Mode	W	$(\rho_0 W^2)'$	$(\rho_0 W^2)$
1	4501	3.704	5.373
2	2827	1.573	2.119
3	4337	−1.663	4.988
7	5732	6.312	8.714
8	4032	1.221	4.312
9	5416	3.683	7.780
10	3306	3.377	2.900
11	3089	−2.812	2.531

hydrostatic-pressure derivatives of the SOEC's were then obtained from

$$(\rho W^2)' = \rho W_0^2 (2f'/f_0 + \chi^T - 2N_k M_m S_{kmii})_{p=0} , \quad (1)$$

where W_0 and f_0 are the mode velocity and the pulse-echo overlap frequency at atmospheric pressure, f' is its pressure derivative, χ^T is the isothermal compressibility, $\mathbf{N}$ corresponds to the wave-propagation direction and S_{IJ} are the elastic compliances. The pressure derivatives $\partial C_{ij}/\partial P$ for the berlinite are compared with those of other rhombohedral crystals in Table V.

The pressure derivatives of the effective bulk modulus for a uniaxial crystal can be written[23] as follows:

$$\begin{aligned} \partial B/\partial P = -2B^2((1/B) + (1/A^2)\{ & A(L - 6 + Q + R) \\ & - S[T(C_{11} + C_{12}) \\ & + U - V]\}) , \end{aligned} \quad (2)$$

where

$$\begin{aligned} B &= 1/(2S_1 + S_3) , \\ A &= C_{33}(C_{11} + C_{12}) - 2C_{13}(C_{33}) , \\ L &= B_{11} + B_{12} - 4B_{13} + 2B_{33} , \\ Q &= (S_2 - 2S_1)(C_{11} + C_{12}) , \\ R &= 2(2S_1 - 3S_3)C_{33} + 4S_3 C_{13} , \\ S &= (C_{11} + C_{12} - 4C_{13} + 2C_{33}) , \\ T &= B_{33} - 1 + (2S_1 - 3S_3)C_{33} , \\ U &= C_{33}[B_{11} + B_{12} + (S_3 - 2S_1)(C_{11} + C_{12})] , \\ V &= 4C_{13}(B_{13} + 1 - S_3 S_{13}) , \\ S_1 &= S_{11} + S_{12} + S_{13} , \\ S_3 &= 2S_{13} + S_{33} . \end{aligned} \quad (3)$$

To express the data in a thermodynamic form suitable for ease of calculating the mode Grüneisen parameter, the hydrostatic-pressure derivatives B_{IJ} (Table V) have been obtained using

$$\begin{aligned} B_{11} &= \partial C_{11}/\partial P - 1 - (S_3 - 2S_1)C_{11} , \\ B_{12} &= \partial C_{12}/\partial P - 1 + (S_1)C_{12} , \\ B_{13} &= \partial C_{13}/\partial P - 1 + (S_1)C_{13} , \\ B_{14} &= \partial C_{14}/\partial P - (S_1)C_{14} , \\ B_{33} &= \partial C_{33}/\partial P + 1 - (S_1 - 2S_3)C_{33} , \\ B_{44} &= \partial C_{44}/\partial P + 1 + (S_1 - 2S_3)C_{44} , \\ B_{66} &= \partial C_{66}/\partial P + 1 + (S_1)C_{66} . \end{aligned} \quad (4)$$

Knowledge of the compression $V(P)/V_0$ (the ratio of volume at a pressure P to that V_0 at atmospheric pressure) is central to any understanding of the behavior of berlinite under pressure. This parameter has been obtained by using the Murnaghan[25] equation which can be usefully used to estimate the volume dependence of crys-

TABLE III. The second-order adiabatic elastic stiffness constants and isothermal compliance constants of berlinite at room temperature (298 K). Units of stiffness 10^{10} $\mathrm{N\,m^{-2}}$, compliance 10^{-11} $\mathrm{m^2N^{-1}}$.

C_{11}	C_{12}	C_{13}	C_{14}	C_{33}	C_{44}	C_{66}	Reference
6.488	0.898	1.460	−1.217	8.714	4.312	2.795	This work
6.344	0.232	0.581	−1.214	5.581	4.315	3.056	5
6.931	1.051	1.349	−1.299	8.862	4.302	2.940	4
6.401	0.724	0.957	−1.235	8.576	4.317	2.838	3
10.500	2.93	6.930	−1.270	13.35	2.310	3.790	8
S_{11}	S_{12}	S_{13}	S_{14}	S_{33}	S_{44}	S_{66}	Reference
1.745	−0.295	−0.243	0.576	1.229	2.644	4.079	This work
1.695	−0.147	−0.154	0.519	1.749	2.609	3.685	5
1.642	−0.321	−0.201	0.593	1.190	2.682	3.925	4
1.731	−0.282	−0.162	0.578	1.202	2.649	4.026	3
1.610	−0.100	−0.890	0.890	1.610	5.300	3.220	8

TABLE IV. Comparison of the elastic constant data of berlinite at 298 K with that of other rhombohedral crystals. The units of the elastic stiffness and compliance constants are 10^{10} N m^{-2} and 10^{-11} m^{2}N^{-1}, respectively.

	Berlinite	Quartz (Ref. 20)	Calcite (Ref. 21)	Bismuth (Ref. 22)	Antimony (Ref. 23)
C_{11}	6.488	8.68	14.52	6.33	10.13
C_{12}	0.898	0.70	5.50	2.45	3.45
C_{13}	1.460	1.91	5.25	2.50	2.92
C_{14}	−1.217	−1.80	−2.03	0.74	2.09
C_{33}	8.714	10.58	8.43	3.80	4.50
C_{44}	4.312	5.82	3.90	1.10	3.93
C_{66}	2.795	3.99	4.52	1.94	3.34
S_{11}	1.745	1.30	1.09	2.61	1.63
S_{12}	−0.296	−0.15	−0.35	−0.80	−0.61
S_{13}	−0.243	−0.30	−0.46	−1.20	−0.66
S_{14}	0.576	0.45	0.75	−2.16	−1.19
S_{33}	1.229	1.02	1.76	4.21	3.09
S_{44}	2.644	2.00	3.35	11.52	3.81
S_{66}	4.079	2.91	2.90	6.79	4.47

tal upon pressures of much greater magnitudes than directly available in ultrasonic experiments:[26]

$$V(P)/V_0=[B_0'P/B_0+1]^{1/B_0'} . \tag{5}$$

Here B_0 and B_0' are the isothermal bulk modulus and its pressure derivative. This equation of state has been used to calculate the relative compression of both materials (Fig. 2), taking as input data the derivatives B_0' equal to 7.410 and 6.33 and isothermal bulk moduli B equal to 3.023×10^{10} N m^{-2} and 4.717×10^{10} N m^{-2} for berlinite and quartz, respectively, in each case. The volume change induced by the application of a given pressure is much larger for berlinite than for quartz—the former material has much less resistance to the volumetric stress.

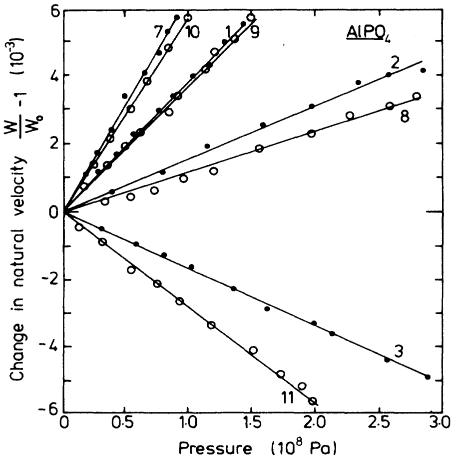

FIG. 1. The relative changes in the natural wave velocity induced by application of hydrostatic pressure to $AlPO_4$. The labeling of the modes is the same as that in Table I.

DISCUSSION

In general the atomic structural arrangement of a material and the strength of its interatomic binding forces determine the elastic behavior of a crystal. Buerger[1] considered the berlinite form of $AlPO_4$ to be a half-breed derivative of quartz, which for comparison can be written as $SiSiO_4$, in which half the Si^{4+} sites are occupied by Al^{3+} and the other half by P^{5+} ions. The space group is $P3_121$ and the point group 32 (Ref. 27). The two crystals have the common feature of containing tetrahedra of oxygen atoms linked together at all the corners with equivalent species, either silicon or aluminum and phosphorus, at the tetrahedron centers. The lattice parameters (nm) are similar, being at 20 °C:[28]

	a	c	c/a
Quartz	0.491 29	0.540 46	1.100
Berlinite	0.494 28	1.097 37	2×1.110

The main difference between the two structures is the doubled c-axis dimension of berlinite due to the different atomic species, aluminum and phosphorus. The bonding is mixed ionic and covalent in character. Using an electric field calculation in a charge-density refinement Thong and Schwarzenbach[2] obtained atomic charges of + 1.4 for Al, + 1.0 for P, and −0.6 for O. The P—O bond is somewhat more covalent than the Al—O bond. As might be anticipated from the structural similarity of the two materials, the elastic moduli of berlinite bear a close formal resemblance to those of quartz (Table IV). In general its smaller elastic constants show that berlinite is signficantly less elastically stiff than quartz, a feature which is consistent with reduced covalent and enhanced ionic contribution to the interatomic binding as compared with quartz. Unlike many other crystals having a uniaxial crystal structure such as arsenic, antimony, or bismuth and consistent with its three-

TABLE V. The hydrostatic-pressure derivatives at 298 K of the effective SOEC (dC_{IJ}/dp) and thermodynamic SOEC (B_{IJ}) of berlinite and other rhombohedral crystals.

	Berlinite present work	Quartz (Ref. 20)	Calcite (Ref. 21)	Bismuth (Ref. 22)	Antimony (Ref. 23)
dC_{11}/dp	8.792	3.28	3.02	6.38	10.8
dC_{12}/dp	12.958	8.66	2.05	2.38	2.9
dC_{13}/dp	3.338	5.97	3.19	4.69	6.7
dC_{14}/dp	2.196	1.93	−1.25	1.70	2.7
dC_{33}/dp	12.235	10.84	2.80	6.62	8.0
dC_{44}/dp	1.663	2.66	0.92	3.37	5.71
dC_{66}/dp	−2.083	−2.69	0.49	2.00	3.90
B_{11}	9.429	5.36	3.59	6.98	11.14
B_{12}	11.908	7.74	0.88	1.44	1.64
B_{13}	2.602	5.05	2.64	4.14	5.80
B_{14}	2.272	1.73	−1.31	1.84	2.67
B_{33}	16.877	12.08	5.47	9.20	10.74
B_{44}	3.443	4.08	2.20	4.58	6.91
B_{66}	−1.240	−1.19	1.35	2.80	4.70

dimensional, oxygen tetrahedral framework, berlinite shows no tendency towards layer like behavior (for example, C_{11} is less than C_{33}). The linear compressibility β, which is a measure of the reduction in the length of a line when a crystal is subjected to hydrostatic pressure, is a useful quantity to consider in relation to elastic anisotropy for a uniaxial crystal. The linear compressiblity in the XY plane β_{XY} ($=S_{11}+S_{12}+S_{13}$) (1.21 for berlinite and 0.85 for quartz) is larger than that β_Z ($=S_{33}+2S_{13}$) along the Z axis, which is 0.743 and 0.42, respectively, for these two materials. Thus both crystals have a markedly anisotropic response to hydrostatic pressure, a line in the XY plane contracting about one and one half times more than one in the Z direction for a given pressure. Hence the effect of hydrostatic pressure is to decrease the a spacing more than the c spacing, driving the c/a ratio further away from 2 for berlinite and from unity for quartz. For crystals with a certain layerlike character, such as the group-V semimetals arsenic, antimony or bismuth, $\beta_Z > \beta_{XY}$. This character is also reflected in the anisotropy of the linear thermal expansion[29–31] which can be very anisotropic in a layerlike crystal so that the Z-direction component α_{33} is substantially larger than α_{11}. In contrast to the layerlike materials, for berlinite (and quartz), α_{11} is greater than α_{33},[32] which is consistent with $\beta_Z < \beta_{XY}$ and $C_{11} < C_{33}$. The excitation of lattice vibrations is easier in the softer directions in the XY plane than along the stiffer Z direction, hence the larger value of S_{11} than S_{33}. This finding is emphasized by the occurrence of negative values of transverse-mode Grüneisen parameters in the XY plane.

Knowledge of the hydrostatic-pressure dependences of the elastic constants (Table V) permits an assessment of the anharmonicity of the acoustic modes in the long-wavelength limit. A physical description of this vibrational anharmonicity is best sought in terms of the Grüneisen parameters in the anisotropic continuum model. Expressions for the zone-center acoustic-mode Grüneisen Γ of rhombohedral crystals in terms of thermodynamic pressure derivatives[33] have been used to compute these parameters for berlinite:

$$\begin{aligned}\Gamma_p^T(\mathbf{N}) = &-(2\omega\beta^T)^{-1}\\ &\times\{1+2\omega[S_1(U_1^2+U_2^2)+S_3U_3^2]-B_{11}(N_1U_1+N_2U_2)^2-B_{66}(N_1N_2-N_2U_1)^2\ ,\\ &\quad -B_{33}N_3^2U_3^2-B_{44}[(N_2U_3+N_3U_2)^2+(N_3U_1+N_1U_3)^2]-2B_{13}(N_1N_3U_1U_3+N_2N_3U_2U_3)\\ &\quad -2B_{14}(N_1^2U_2U_3+2N_2N_3U_1U_3+2N_1N_3U_1U_2-N_2^2U_2U_3+N_2N_3U_1^2-N_2N_3U_2^2)\}\ ,\end{aligned}$$

where

$$\begin{aligned}\omega = &\,C_{11}(N_1U_1+N_2U_2)^2+C_{66}(N_1U_2-N_2U_1)^2+C_{33}N_3^2U_3^2+C_{44}[(N_2U_3+N_3U_2)^2+(N_3U_1+N_1U_3)^2]\\ &+2C_{13}(N_1N_3U_1U_3+N_2N_3U_2U_3)\\ &+2C_{14}(N_1^2U_2U_3+2N_1N_2U_1U_3+2N_1N_3U_1U_2-N_2^2U_2U_3+N_2N_3U_1^2-N_2N_3U_2^2)\ . \end{aligned} \tag{6}$$

Essentially as a consequence of the negative pressure derivative $\partial C_{66}/\partial P$ (Table V), Grüneisen Γ for shear modes are negative over quite a large range of propagation directions (Fig. 3). Usually elastic constants and lattice vibrational frequencies increase under hydrostatic pressure so that the mode Grüneisen parameters are positive. All the longitudinal and quasilongitudinal modes show this normal behavior with the Grüneisen parame-

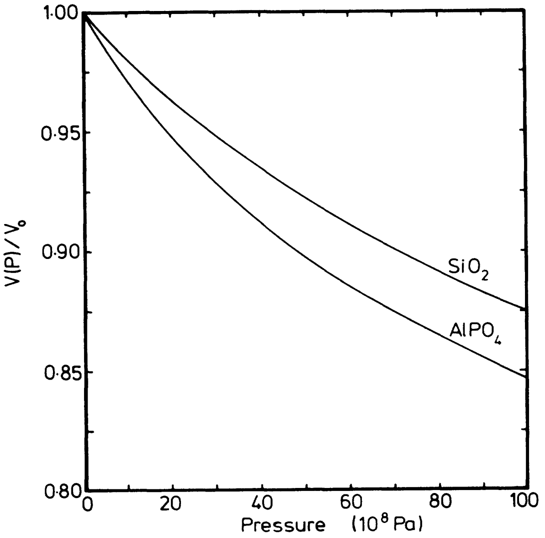

FIG. 2. The compressions of berlinite and quartz, extrapolated to high pressure using the Murnaghan equation of state.

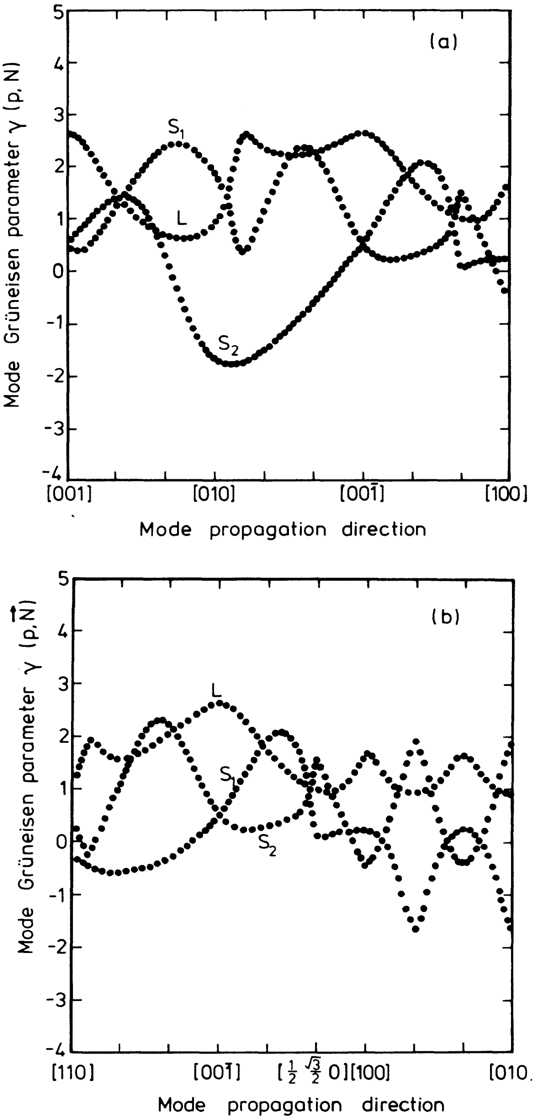

FIG. 3. The Brillouin-zone center, acoustic-mode Grüneisen parameters of berlinite as a function of mode propagation direction.

ters ranging between 0.624 and 2.65, the largest value being associated with the pure longitudinal mode propagating along the Z axis, the direction of strongest bonding.

Aluminium phosphate undergoes an α-β displacive transformation which closely resembles that in quartz. At T_0 equal to about 853 K inclusion of 180° rotational symmetry about the Z axis takes the trigonal α form berlinite (point group 32) to the hexagonal β form (point group 622).[11] The transformation to β is not direct; in the transition region a spatially inhomogeneous state[34] of incommensurate type exists.[35–37] Raman spectra studies[12,13] show that as the temperature is increased towards T_0 an optic-phonon mode softens at the Γ point from its room-temperature wave number ($\sim$220 cm^{-1}); at high temperature a one-phonon anharmonic coupling ensues by Fermi resonance with a state at 158 cm^{-1}. In the context of Landau theory[38] the α-β structural change involves a symmetry breaking which is consistent with a second-order transition. For quartz the tilt angle of the SiO_4 tetrahedra about their twofold axis can be taken as the order parameter.[39] For berlinite the measured changes in atomic positions with increasing temperature indicate that as the transition is approached the PO_4 and AlO_4 tetrahedra rotate around a binary axis and that there is also a relative translation along this axis.[14,15] The tilt of the tetrahedra about their binary axis reverses in a sense at about 40 K below T_0 before changing continuously to the β-phase orientation. The tilt angle by itself is not an acceptable order parameter.[15] In spite of this unresolved difficulty it is clear that optic-phonon mode softening constitutes the driving mechanism of the transition.

To proceed to find out how this optic-phonon mode softening might influence elastic stiffness, it is useful to return to consider the situation in quartz, which is better understood. The transition in quartz is nearly second order in character and is driven by a zone center soft optic phonon with an energy of 25.8 meV (207 cm^{-1}) at room temperature.[40] Above the transition inelastic scattering shows the critical behavior expected for a soft-phonon mode. The eigenvectors for this soft mode correspond closely to the atomic displacements appropriate to the structural change. Crystallographic and neutron scattering studies for quartz have been made in the hexagonal-system reference frame, while all the elastic-constant work (including this study of berlinite; see experimental procedure and results) has been referred to the IRE standard[17] which is the X,Y,Z axial set in the trigonal system. The phonons which are central to discussion of the mode softening have wave vectors parallel to $[\zeta 00]$ (Ref. 41) in the hexagonal reference frame and will be denoted $[\zeta 00]_H$; their direction of

TABLE VI. A collection of Grüneisen parameters and thermal expansion (in units of 10^{-5} K^{-1}) data for rhombohedral crystals in the high-temperature limit ($T > \Theta_D$). Data are extracted from various tables given in Ref. 15. The thermal expansion data for $\mathrm{AlPO_4}$ are taken from Ref. 32.

	$\gamma_{\parallel}^{\mathrm{el}}$	$\gamma_{\perp}^{\mathrm{el}}$	$\gamma_{\parallel}^{\mathrm{th}}$	$\gamma_{\perp}^{\mathrm{th}}$	α_{33}	α_{11}
Quartz	−0.16	0.26	0.96	1.18	0.80	1.30
Calcite	0.87	−0.13			2.51	−0.49
Bismuth	1.90	0.20	1.10	1.32	1.7	1.14
$\mathrm{Al_2O_3}$	0.54	0.39	0.48	0.43	0.57	0.50
$\mathrm{LiNbO_3}$	−0.31	0.05			0.75	1.54
$\mathrm{AlPO_4}$			0.646	0.649	1.59	0.97

propagation corresponds to the Y direction in the trigonal system which is used to define the ultrasonic-mode propagation directions and elastic-stiffness relationships of Table I. X-ray measurements[11,42] show strong diffuse scattering along the $[\zeta 00]_H$ direction of α quartz. Now neutron inelastic scattering studies have shown that softening of the optic phonons occurs predominantly in the $[\zeta 00]_H$ direction[41] and is the origin of the strong x-ray diffuse scattering along this direction. In the quartz structure there is only one irreducible representation for phonons with wave vector **q** along the $[\zeta 00]_H$ direction; one phonon branch cannot cross another so as the optic branch softens it depresses the transverse-acoustic branch in this direction. In the long-wavelength limit the slope of this depressed acoustic branch is given by

$$\omega/q=(C_{66}/\rho)^{1/2} .$$

The measured value of C_{66} for α quartz is consistent with the calculated depression of this acoustic branch for wave vector **q** close to the zone center;[41] C_{66} shows an anomalous increase with temperature and $\partial C_{66}/\partial P$ has a negative value (Table V) which is often indicative of acoustic-mode softening. Since the α-β transition in berlinite has a close structural affinity with that in quartz, it can be anticipated that anharmonic coupling of the soft optic mode to the transverse acoustic mode should also occur and that the behavior of C_{66} should reflect this. It does. C_{66} increases with temperature and $\partial C_{66}/\partial P$ is anomalously negative (Table V). In both materials the transverse-acoustic branch having modes propagating normal to the binary direction in the plane normal to the threefold rotational axis show unusual behavior of the elastic constant C_{66} with pressure which is consistent with pressure-induced mode softening at the long-wavelength limit. Negative mode Grüneisen parameters, which imply a decrease in the energy of the mode under pressure, are indicative of incipient lattice instability.[10] The long-wavelength acoustic shear mode Grüneisen parameters of berlinite are negative for certain crystallographic directions most markedly in a core of directions centered on the Y ([010]) direction (Fig. 3). This is consistent with the predictions of the soft-mode theory and suggests that even far below the phase-transition temperature there could already be a degree of anharmonic coupling between the strain and the order parameter.

The anharmonicity of the lattice vibrations is responsible for thermal expansion α of a material, as well as the nonlinear acoustic behavior under a finite stress. The thermal Grüneisen parameter γ^{th} (See Table VI)

$$\gamma^{\mathrm{th}}=3\alpha B^{s}/\rho C_P$$

is a thermodynamic quantity often used to describe anharmonicity; in the quasiharmonic approximation it can be determined from a weighted mode average of the mode Grüneisen parameters $\gamma_i=-(\partial \ln\omega_i/\partial \ln V)$,

$$\gamma^{\mathrm{th}}=\sum_i C_i\gamma_i \Big/ \sum_i C_i .$$

For a noncubic crystal γ^{th} is a second-rank tensor property, and for a rhombohedral crystal its two independent components are given by

$$\gamma_{XY}=[(C_{11}+C_{12})\alpha_{11}+C_{13}\alpha_{33}]V/C_P ,$$

$$\gamma_Z=(2C_{13}\alpha_{11}+C_{33}\alpha_{33})V/C_P ,$$

where C_P is the specific heat at constant pressure ($=93.222$ $\mathrm{J\,mol^{-1}\,K^{-1}}$) (Ref. 43). γ_{XY} has been determined to be 0.649 and γ_Z is equal to 0.646 in the high-temperature limit T ($>\Theta_D$). The mean long-wavelength acoustic-mode Grüneisen parameters $\gamma_{XY}^{\mathrm{el}}$ ($=0.487$) and γ_Z^{el} ($=1.227$) are quite different. In the high-temperature limit the thermal Grüneisen parameters include contributions from all branches of the phonon spectrum and all wave vectors throughout the acoustic and optic branches which should account for the differences between the components of γ^{el} and γ^{th}.

To conclude, for berlinite the elastic constants and their hydrostatic-pressure derivatives have a similar pattern to those of quartz. Berlinite is less stiff elastically than quartz. Its smaller pressure derivatives show that application of pressure does not result in an increase of the stiffness of berlinite as strongly as in the case of quartz. Both crystals respond anisotropically to pressure in a similar manner: a line in the XY plane contracts rather more for a given pressure than one in the Z direction. Again like quartz, berlinite has a negative-pressure derivative $\partial C_{66}/\partial P$, and the long-wavelength transverse acoustic-mode Grüneisen parameters are negative for propagation directions centered around the Y axis. This behavior is consistent with interaction between the transverse-acoustic phonon branch and the optic branch in the same crystallographic Y direction, softening of these particular optic phonons being responsible for the α-β structural transformation which takes place at elevated temperatures.

*Permanent address: Department of Physics, Agriculture University of Malaysia, 43400 Serdang, Selangor, Malaysia.

†Permanent address: Institute of Crystal Materials, Shandong University, Jinan Shandong, People's Republic of China.

[1] M. J. Buerger, Am. Mineral. **33**, 751 (1948).

[2] N. Thong and D. Schwarzenbach, Acta Cryst. **A35**, 658 (1979).

[3] Z. P. Chang and G. R. Barsch, IEEE Trans. Sonics Ultrason. **23**, 127 (1976).

[4] D. S. Bailey, W. Soluch, D. L. Lee, J. F. Vetelino, and J. Andle, Proceedings of the 36th Annual Frequency Control Symposium, (unpublished).

[5] Wang Hong, Xu Bin, Liu Xiling, Han Jianru, Shan Shuxia, and Li Hu, Proceedings of the Eighth International Conference of Crystal Growth, 1986 (unpublished); J. Cryst. Growth **227**, 1 (1986).

[6] R. M. O'Connell and P. H. Carr, IEEE Trans. Sonics Ultrason. **24**, 6 (1977).

[7] D. Schwarzenbach, Z. Kristallogr. Kristallgeom. Kristallphys. Kristallchem. **123**, 161 (1966).

[8] W. P. Mason, *Piezoelectric Crystals and Their Application to Ultrasonics* (Van Nostand, New York, 1950); p. 208.

[9] M. Born and K. Huang, *Dynamical Theory of Crystal Lattices* (Oxford University, New York, 1954).

[10] E. Chang and G. R. Barsch, J. Phys. Chem. Solids **34**, 1543 (1973).

[11] H. Arnold, Z. Kristallogr. Kristallgeom. Kristallphys. Kristallchem. **121**, 145 (1965).

[12] J. F. Scott, Phys. Rev. Lett. **24**, 1107 (1970).

[13] J. F. Scott, Phys. Rev. B **4**, 1360 (1971).

[14] H. N. Ng and C. Calvo, Can. J. Phys. **54**, 638 (1976).

[15] R. Lang, C. Calvo, and W. R. Datars, Can. J. Phys. **55**, 1613 (1977).

[16] J. Detaint, H. Poignant, and Toudic, Proceedings of the 34th Annual Frequency Control Symposium USAERADCOM, Ft. Monmouth, New Jersey, 1980 (unpublished).

[17] IRE Standards on Piezoelectric Crystal [Proc. IRE **46**, 764 (1958); **37**, 1378 (1949)].

[18] H. E. Swanson, M. I. Cook, E. H. Evans, and J. H. De Groot, *Standard X-ray Diffraction Powder Patterns,* Nat. Bureau Standards (U.S.) Circ. No. 539 (U.S. GPO, Washington, D.C., 1960), Vol. 10, p. 3.

[19] E. P. Papadakis, J. Acoust. Soc. Am. **42**, 1045 (1967).

[20] H. J. McSkimin, P. Andreatch, and R. N. Thurston, J. Appl. Phys. **36**, 1624 (1965).

[21] H. Kaga, Phys. Rev. **172**, 900 (1968).

[22] Tu Hailing and G. A. Saunders, Phil. Mag. A **48**, 4 (1983); **48**, 451 (1983).

[23] G. A. Saunders and Y. K. Yoǵurtçu, Phys. Rev. B **30**, 10 (1984); **30**, 5734 (1984).

[24] R. N. Thurston and Brugger, Phys. Rev. **133**, A1604 (1964); **135**, AB3(E) (1964).

[25] F. D. Murnaghan, Proc. Nat. Acad. Sci. USA **30**, 244 (1944).

[26] O. L. Anderson, J. Phys. Chem. Solids **27**, 547 (1966).

[27] B. Sharan and B. W. Dutta, Acta Cryst. **17**, 82 (1964).

[28] E. Knolmayer, Proceedings of the 34th Annual Frequency Control Symposium, Ref. 16.

[29] G. V. Bunton and S. Weintraub, J. Phys. C **2**, 116 (1967).

[30] N. G. Pace and G. A. Saunders, J. Phys. Chem. Solids **32**, 1585 (1971).

[31] G. K. White, J. Phys. C **5**, 2731 (1972).

[32] J. B. Austin, H. Salni, and R. H. H. Pierce, Phys. Rev. **57**, 931 (1940).

[33] Tu Hailing and G. A. Saunders, J. Mat. Sci. **18**, 2337 (1983).

[34] G. van Tendeloo, J. van Landuyt, and S. Amelinckx, Phys. Status Solidi A **33**, 723 (1976).

[35] T. A. Aslanian and A. P. Levanuk, Solid State Commun. **31**, 547 (1979).

[36] D. J. Durand, M. Lopez, L. Cot, O. Retout, and P. Saint-Gregoire, J. Phys. C **16**, L311 (1983).

[37] P. Saint-Gregoire, F. J. Schafer, W. Kleemann, J. Durand, and A. Goiffon, J. Phys. C **17**, 1375 (1984).

[38] L. D. Landau and E. M. Lipshitz, *Statistical Physics* (Pergamon, London, 1958), Chap. XIV.

[39] H. Grimm and B. Dorner, J. Phys. Chem. Solids **36**, 407 (1975).

[40] J. D. Axe and G. Shirane, Phys. Rev. B **1**, 342 (1970).

[41] K. H. W. Bauer, H. J. Agodzinski, B. Dorner, and H. Grimm, Phys. Status Solidi B **48**, 437 (1971).

[42] R. Comes, M. Lambert, and A. Guinier, Acta Cryst. A **26**, 244 (1970).

[43] D. D. Wagman, W. H. Evans, V. B. Parker, I. Harlow, S. M. Bailey, and R. H. Schumm, *Selected Values of Chemical Thermodynamic Properties* Circ. No. 270-3 (U.S. GPO, National Bureau of Standards (U.S.) Washington, D.C., 1968), p. 215.